Simultaneous Determination of Quantum Efficiency and Energy Efficiency of Semiconductor Photoelectrochemical Cells by Photothermal Spectroscopy

Akira Fujishima,* Yasuhisa Maeda, and Kenichi Honda

Department of Synthetic Chemistry, Faculty of Engineering, The University of Tokyo, Hongo, Tokyo 113, Japan

and George H. Brilmyer and Allen J. Bard***

Department of Chemistry, The University of Texas at Austin, Austin, Texas 78712

ABSTRACT

During a photoelectrochemical reaction only a portion of the light energy absorbed by the semiconductor (CdS or TiO_2 single crystal) is utilized in the electrode reaction. The unused portion of energy is expended through various mechanisms as heat. Therefore by monitoring temperature changes within the photoanode as a function of electrode potential and light intensity, information concerning the efficiency of the process can be obtained. Experimental results are presented and interpreted using a model for the energy balance within the system. This permits the determination of the quantum and energy efficiencies simultaneously without the need to calibrate the light source.

A number of photoelectrochemical cells based on semiconductor electrodes for photoelectrosynthesis (*e.g.*, the photodecomposition of water) and the conversion of solar energy to electricity have been reported (1-15). The major factors determining the efficacy of these semiconductor electrode cells are the quantum efficiency for electron flow (*i.e.*, number of electrons flowing/number of photons absorbed), and the power conversion efficiency (*i.e.*, chemical or electrical power output/input radiant power). It is not uncommon to find near unity quantum yields for electron flow at a sufficiently high bias (positive for the case of n-type semiconductors) during irradiation with greater than bandgap energy light for many semiconductors. However, even when high quantum efficiencies have been obtained, the power efficiencies were much lower (10-15). For example, for photooxidation at a CdS single crystal anode, Wrighton *et al.* (15) reported that with an Se^{2-} solution the maximum monochromatic power efficiency obtained was 3.4% with a maximum quantum efficiency of 49%. Such findings demonstrate that the major part of the light energy absorbed by the semiconductor is not used for the photo-assisted oxidation but rather is converted to heat energy probably via radiationless transitions within the conduction band of the semiconductor (*i.e.*, when the photon energy is in excess of the bandgap energy) or electron-hole recombination processes. Consequently, thermal measurements of the semiconductor electrode during electrolysis can aid in the determination of the efficiencies and perhaps in the elucidation of the mechanism of the cell processes.

We recently described a new spectroscopic method called Photothermal Spectroscopy (PTS) (16). This technique involves placing a thermistor on or in close proximity to a sample and measuring temperature changes (*i.e.*, thermistor resistance changes) during sample irradiation with monochromatic light. This technique can be easily adapted to cases when the sample is a semiconductor electrode (17). Cahen (18) has also shown that similar measurements with photoacoustic spectroscopy can be used to determine the efficiency of solid-state photovoltaic devices. We report in this paper measurements of the conversion of light energy to chemical and/or electrical energy at CdS and TiO_2 photoanodes by direct determination of the temperature changes of semiconductor electrodes. The results were interpreted using a theoretical equation for the energy balance within the system. In this manner the quantum efficiency and power efficiency could be determined without calibration of the irradiation source.

* Electrochemical Society Active Member.
** Electrochemical Society Student Member.
Key words: photoelectrochemical, semiconductor electrode, quantum efficiency, energy efficiency, temperature changes.

Experimental

Procedure.—The basic photothermal experiment was essentially carried out as previously described with slight modifications (16, 17). In these experiments the photoanodes studied were CdS and TiO_2 single crystals. The results reported here are for monochromatic radiation at wavelengths corresponding to energies greater than the bandgap energy (for example, for CdS, 490 nm). The photothermal responses were obtained for the photoanodes during both anodic polarization and under open-circuit conditions in the electrolyte solutions. The corresponding current and temperature changes were then plotted as a function of potential. Experiments were carried out in two laboratories with two different experimental setups (referred to as A and B).

Instrumental.—Block diagrams of these are shown in Fig. 1 and 2. The apparatus (A) in Fig. 1 employed a 500W high pressure mercury lamp (Ushio Electric Company Limited) housed in an Ushio Model UI-501C housing. A lens was used to focus the light beam and interference filters (Koshin Kogaku Company Limited) were employed to select the wavelength of exciting light. A shutter with two timers, made by special order for this experiment (Ishikawa Seisakusho Company Limited) was used to fix precisely the irradiation period. System B is shown in Fig. 2. The light source was a 2500W short arc xenon lamp housed in an Oriel Model LH-152N housing. The output of the lamp was first chopped mechanically (on 20 sec; off 40 sec) and then focused using f/1 quartz optics on the entrance slit of a Jarrell-Ash Monochromator (Model 82-410). The resulting monochromatic light (10 nm bandpass) was then filtered of second order and finally focused on the photoanode within the electrochemical cell.

All cells were equipped with platinum counter-electrodes and saturated calomel reference electrodes (SCE). Irradiation was accomplished through optically flat windows both in the water baths and in the cells. The working electrodes were placed a sufficient distance from the cell window (~2 cm) to avoid any

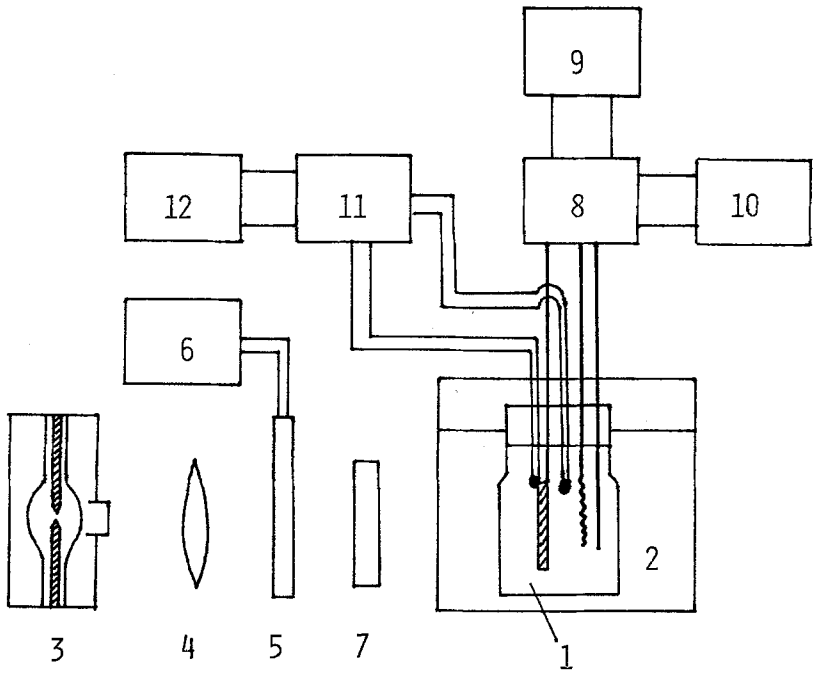

1; CELL 2; WATER BATH
3; 500W H_g LAMP 4; LENS
5; SHUTTER 6; TIMER
7; FILTER 8; POTENTIOSTAT
9; POTENTIAL SWEEPER 10; X-Y RECORDER 11; D.C. BRIDGE
12; POLYRECORDER

Fig. 1. Measurement assembly, A

heating effects due to window heating. A nitrogen bubbler was employed for deoxygenating the solutions. The cell temperature was maintained by a water bath which in System A was thermostatted.

The working electrodes were cadmium sulfide single crystals [(001) surface] (Teikoku Tsushin Company Limited) which had dimensions 10 × 10 × 1 mm and a carrier density of 4.8×10^{16} cm^{-3}, and titanium dioxide single crystals [(001) surface] (Nakazumi Crystal Company Limited) each having dimensions about 10 × 10 × 1.5 mm and treated by reduction to increase carrier density. The ohmic contacts were made by electroplating indium on one side of each crystal and then attaching a copper wire to the contact with conducting silver epoxy [Seisin Shoji Company Limited, No. 4992 (A), or Allied Products Corporation, New Haven, Connecticut (B)]. The back and sides of the crystal were insulated and mounted on a flat piece of glass attached to a glass rod with epoxy resin [Semedian Company Limited (A), or Devcon Incorporated, Danvers, Massachusetts (B)]. The semiconductor surfaces were polished with 0.3 μm polishing alumina prior to use. Then, in the case of CdS they were etched just before use in concentrated hydrochloric acid for 10 sec.

The structure of the semiconductor electrode (with a thermistor in place) is shown in Fig. 3. Matched pairs of thermistors were used: (A) Shibaura Electronics Model BSB4-41A; nominal resistance 4 kΩ sensitivity, 0.052°C/Ω or (B) Victory Engineering Incorporated, Model 32A223; nominal resistance, 2 kΩ, sensitivity, 0.013 °C/Ω. Both had time constants of 0.4 sec when immersed in unstirred water. The thermistors were used in a differential arrangement with one thermistor held against the front surface of the electrode and the other positioned behind the electrode while not touching it. The cell was carefully positioned so that the monochromatic light beam struck the whole exposed surface of the electrode but neither of the thermistors. Thus a change in temperature of the electrode caused a resistive change in the thermistor and produced a voltage imbalance in (A) the d-c or (B) the a-c bridges. This small voltage was amplified and then displayed on strip chart re-

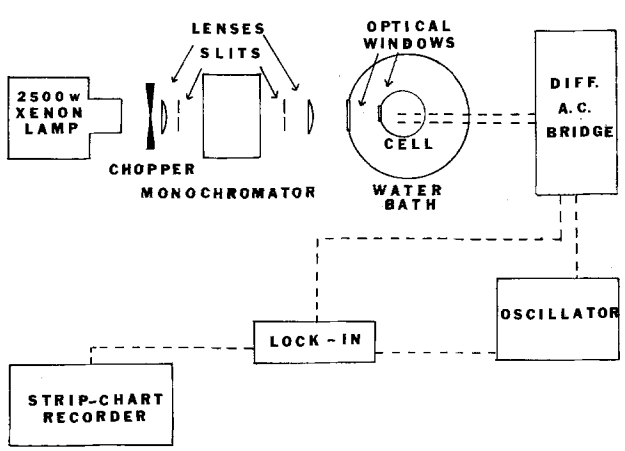

Fig. 2. Measurement assembly, B

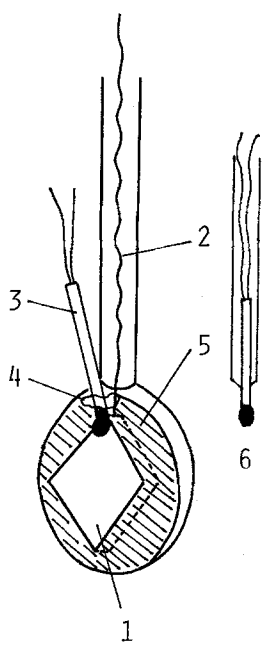

1; SEMICONDUCTOR CRYSTAL
2; C_u LEAD WIRE
3; THERMISTOR
4; SILICONE RUBBER
5; EPOXY RESIN
6; REFERENCE THERMISTOR

Fig. 3. Structure of semiconductor electrode. Light irradiates only the semiconductor surface and not the thermistors. The contact to the electrode and the thermistor is insulated from the solution by a thin layer of epoxy cement.

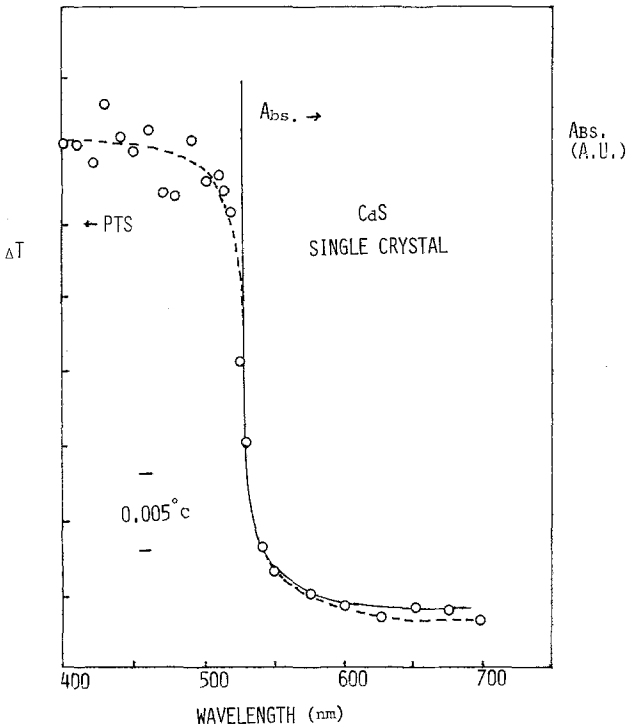

Fig. 4. Photothermal spectrum (PTS) of CdS single crystal. The solid line shows the absorption spectrum of the same crystal.

corders (A) Tao Electronics Model ERP-2T or (B) Tosely Model 7100B.

The current-potential and current-time curves were measured under potentiostatic conditions using potentiostats and potential programmers: (A) Nikko Keisoky Company Limited (Models NRGS-301 and NPS-2) and (B) Princeton Applied Research (Models 173 and 175). Cyclic voltammograms and current-time curves were displayed on an X-Y recorder [(A) Yokokawa Type 3078 or (B) Houston Instruments Model 2000].

The monochromatic lamp intensity was measured precisely using either (A) a chemical actinometric method (potassium ferrous oxalate) or (B) an EG&G radiometer/photometer Model 550-1. All chemicals were of reagent grade and were used without further purification.

Results

Previous studies with photothermal spectroscopy (PTS) have shown that the temperature changes which occur upon light absorption correlate well with the results of optical absorption spectroscopy. This is demonstrated in the PTS of single crystal CdS (Fig. 4) where irradiation with light of energy greater than the bandgap produces electron-hole pairs which, if the semiconductor is not a fluorescent, phosphorescent, or photochemically active material, recombine through radiationless transitions to produce heat. Although the spectrum shown in this figure was observed for the sample in air, similar PTS spectra of smaller magnitude were measured in water. The magnitude of the observed signal depends on the thermal conductivity and the heat capacity of the sample and its environment.

When an n-type semiconductor is used as a photoanode of a photoelectrochemical cell, that portion of the impinging radiant energy which is not converted to electrical energy or stored as chemical energy is dissipated as heat. One source of this heat is the difference between the photon energy, E $(=h\nu)$, and the bandgap energy, E_g; this represents radiationless processes within the conduction band after light absorption. Other factors leading to heat dissipation are the difference between the valence band energy level and the solution redox level, $|E_{VB} - E_{redox}|$ and the difference (usually small) between the Fermi level and conduction band level, $|E_{F,\,flatband} - E_{CB}|$. Note that even when the quantum efficiency is unity, dissipation caused by these factors will cause heating at the electrode surface.

$CdS/Fe(CN)_6^{3-}$, $Fe(CN)_6^{4-}$ system.—The photothermal experiment was applied to the photo-oxidation of $K_4Fe(CN)_6$ at the CdS photoanode. The solution used was 0.1M $K_4Fe(CN)_6$, 0.001M $K_3Fe(CN)_6$, and 0.2M Na_2SO_4 as the electrolyte. Current-potential curves using the CdS electrode showed typical behavior of an n-type semiconductor electrode ($V_{FB} = -1.0$V *vs.* SCE). The quantum efficiency of the CdS crystal was calculated to be nearly 100%, when the crystal was irradiated with greater than bandgap light (490 nm) (which was not absorbed by the electrolyte solution) and the electrode maintained at 2.0V *vs.* SCE. When the crystal was used as a photoanode in the solution, there was no change in photocurrent with time and no sulfur was detected on the surface after prolonged use. Therefore, we conclude that the $K_4Fe(CN)_6$ was the species oxidized and that the photoanode was stable in this solution.

The changes in temperature *vs.* time were measured at each applied potential while the photocurrent was recorded simultaneously. In the dark, no change in temperature was observed either at open circuit or at potentials positive of V_{FB}, where the observed currents were less than 10^{-9} A/cm². Figure 5 illustrates typical changes in temperature with time upon irradiation with greater than bandgap light (490 nm) at open-circuit condition and with various applied potentials. The temperature increased almost linearly when the light pulse was initiated. When the light pulse was terminated (after 20 sec irradiation) the temperature decreased quickly. We have already dis-

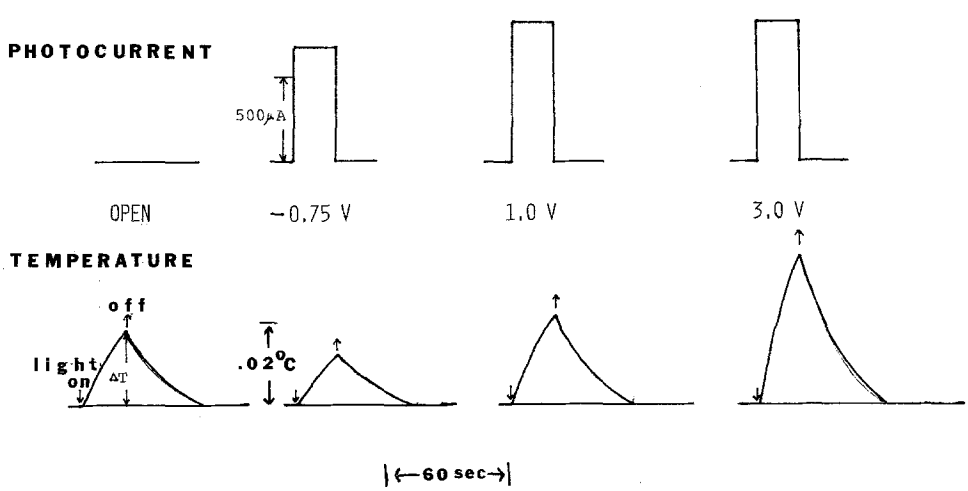

Fig. 5. The change in temperature *vs.* time for the CdS anode in 0.1M $K_4Fe(CN)_6$, 0.001M $K_3Fe(CN)_6$, and 0.2M Na_2SO_4. Upper curves show the anodic photocurrent *vs.* time.

cussed this behavior in the simplified theory of PTS (16).

In Fig. 6 the temperature change *vs.* potential and the corresponding photocurrent-potential curves are experimentally plotted. These results are representative of those obtained with both systems. Compared with the heating observed at open circuit, the temperature increase was smaller at −0.5V and larger at 2.0V and 4.0V, respectively.

TiO_2/H_2SO_4 system.—As the TiO_2 photoanode, three different TiO_2 single crystals were used. Each was reductively treated under vacuum at various temperatures and for different lengths of time: (*i*) 3 hr at 650°C; (*ii*) 3 hr at 550°C; (*iii*) 4 hr at 800°C. The experiments were conducted using each TiO_2 single crystal electrode in a 1M sulfuric acid solution. Since the bandgap of TiO_2 is 3.0 eV, the wavelength of the light chosen for irradiation was 370 nm. The irradiation period was fixed at 20 sec in each case. The results of a typical experiment using the first (and most efficient) TiO_2 electrode are shown in Fig. 7. The three different crystals showed quite different slopes for the temperature increase *vs.* potential curves. The semiconductor electrode which produced the largest photocurrent showed the steepest slope.

Theoretical Treatment

The experimental results can be interpreted by considering the energy balance within the photoelectrochemical cell. The first aspect of this formulation will be to examine a simple electrochemical reaction from a thermodynamic point of view to determine what information concerning the system can be obtained via thermal measurements. This model will then be modified to fit the constraints of the photoelectrochemical system which is slightly more complex yet very similar. The resulting thermal relationships will then be used to investigate the quantitative aspects of various photoelectrochemical devices.

Calorimetry has been used by previous investigators to measure the enthalpy change (ΔH_c) which occurs during an electrochemical reaction (19). Such a system can be described by the equation

$$\Delta H_c = Q - W_e \qquad [1]$$

where W_e is the electrical work into (or out of) the system and Q is the heat evolved in the system from reversible and irreversible work. The electrical work can be expressed in terms of current, voltage, and

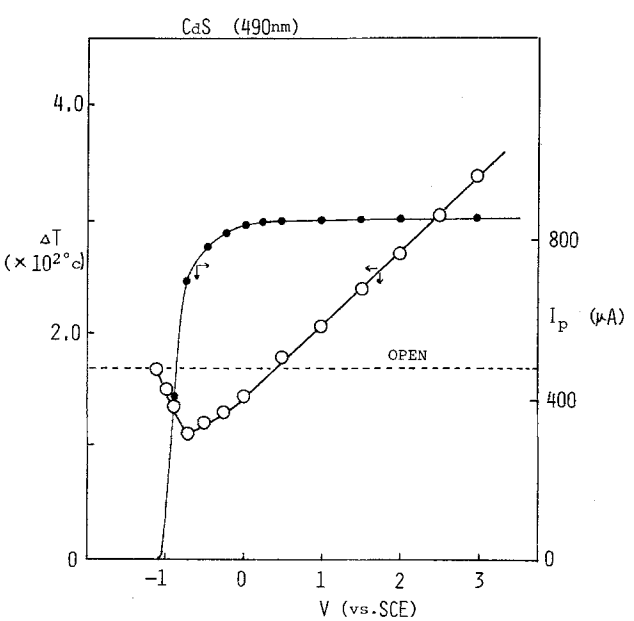

Fig. 6. Temperature change *vs.* potential (○) and photocurrent *vs.* potential (●) of the CdS single crystal electrode.

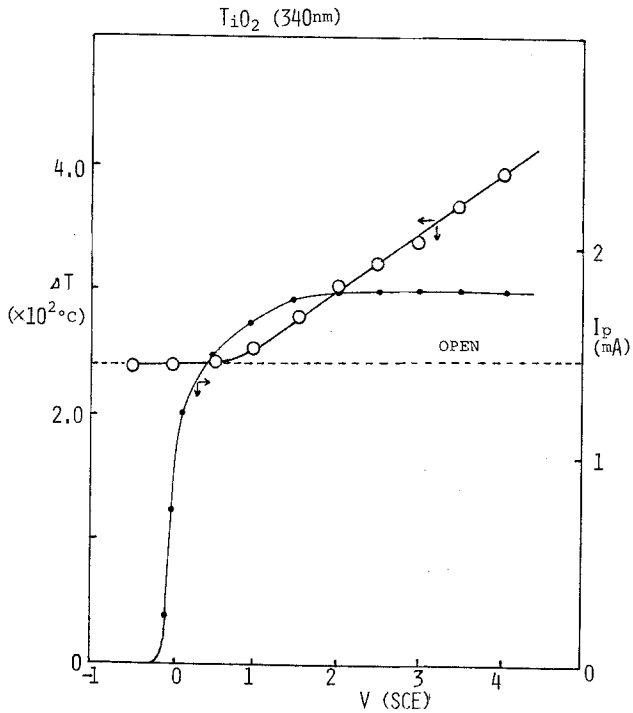

Fig 7. Temperature change *vs.* potential (○) and photocurrent *vs.* potential (●) of the TiO_2 single crystal electrode. TiO_2 single crystal was treated in the vacuum for 3 hr at 650°C.

time (Vit) and the heat evolved in terms of an entropy change for the whole cell reaction ($T\Delta S$), activation energy, in terms of overpotential, η, (ηit) and the contribution from electrode and solution resistance, R, (i^2Rt). The total expression for the enthalpy is thus

$$\Delta H_c = T\Delta S + \eta it + i^2Rt - Vit \qquad [2]$$

This equation is directly applicable to the photoelectrochemical situation by considering two additional energy terms and by reevaluating the electrochemical cell in terms of energy in and out.

For the case of a photoelectrochemical device one must now consider that the electrode is illuminated with a monochromatic light pulse having an energy E (eV/photon), with an average absorbed intensity I (photon/sec) for a time t (sec). Therefore the total energy put into the system per light pulse is EIt (eV). This energy can then either be used by the semiconductor to promote the electrode reaction with production of electrical work (Vit) or evolved as heat in the semiconductor (Q_{sc}) via recombination and other radiationless processes. The resulting equation for the overall photoelectrochemical reaction is

$$\Delta H_c = Q_T - W_T \qquad [3]$$

where

$$Q_T = T\Delta S + \eta it + i^2Rt + Q_{sc} \qquad [4]$$

$$W_T = EIt + Vit \qquad [5]$$

therefore

$$\Delta H_c = T\Delta S + \eta it + i^2RT + Q_{sc} - EIt - Vit \qquad [6]$$

Upon rearrangement the relationship between the measured quantity, Q_T, and the rest of the variables we obtain

$$Q_T = Q_{sc} + T\Delta S + \eta it + i^2RT = EIt + Vit + \Delta H_c \qquad [7]$$

This final equation can now be related to the actual photoelectrochemical experiment. Although determination of Q_T by calorimetric means is possible, in the photothermal experiments relative temperature changes are measured and these are used to extract the desired information. This is done by comparing Q_T

measured during current flow in the photoelectrochemical experiment to that measured when the cell is at open circuit. In the open circuit case no net electrochemical reaction occurs and all the absorbed light energy is converted to heat, Q^{o}_{T}, within the semiconductor, so that

$$Q^{o}_{T} = Q_{sc} = EIt \quad [8]$$

This condition shows that the heat absorbed by the system is directly proportional to the light energy put into this system. Therefore

$$\frac{Q_T}{Q^{o}_{T}} = \frac{Q_{sc} + T\Delta S + \eta it + i^2RT}{EIt} \quad [9]$$

The corresponding relative change in temperature at the semiconductor surface can be represented by

$$\frac{\Delta T}{\Delta T^{o}} = \Delta T_{rel} = \frac{Q_{sc} + T\Delta S + \eta it + i^2RT - k\Delta T}{EIt - k\Delta T^{o}} \quad [10]$$

where $k\Delta T$ is the heat lost by conduction from the electrode. Several assumptions must be made at this point concerning these temperature measurements. The first and most important is that temperature changes occurring on the electrode surface both in the semiconductor (Q_{sc}) and in solution ($T\Delta S + \eta it + i^2Rt$) are equally detectable. This is a good assumption because in general, the thermal conductivity of the electrode is at least an order of magnitude greater than that of the solvent. Other assumptions which must be made to simplify the treatment are that the terms $k\Delta T$ and i^2RT are very small and can therefore be neglected. This is acceptable because the temperature changes measured are typically on the order of millidegrees and the total resistance is usually very low. Note that if the $k\Delta T$ terms are not negligible, corrected values of ΔT can be obtained by extrapolation of the initial linear portion of the temperature rise with time to the value ΔT_{corr} at the time when the temperature begins to fall. In the activation term the overpotential, η, is actually $V - V_{FB}$ (where V_{FB} is the flatband potential of the semiconductor) so that Eq. [10] can be written as

$$\frac{\Delta T}{\Delta T^{o}} = \frac{Q_{sc} + T\Delta S}{EIt} + \frac{i(V - V_{FB})}{EI} \quad [11]$$

The left side of the equation can be given specific energy units to facilitate the mathematical treatment to finally yield

$$E\frac{\Delta T}{\Delta T^{o}} = \frac{Q_{sc} + T\Delta S}{It} + \eta_q(V - V_{FB}) \quad [12]$$

where $\eta_q = i/I$ = quantum efficiency of the photooxidation and $(Q_{sc} + T\Delta S)/It$ is the total heat change (usually evolved) in the system (at the photoanode). Therefore under constant illumination conditions (*i.e.*, EIt held constant) a plot of $E\frac{\Delta T}{\Delta T^{o}}$ against $(V - V_{FB})$ yields the quantum efficiency, η_q, from the slope of the straight line and the loss term, $(Q_{sc} + T\Delta S)/It$, is obtained from the intercept of the $E\frac{\Delta T}{\Delta T^{o}}$ axis at $V = V_{FB}$ as shown in Fig. 8. We define the single electrode, monochromatic energy efficiency of the system as

$$\eta_e = \frac{EIt - Q_{sc}}{EIt} \times 100 \quad [13]$$

The efficiency as defined above can then be obtained by making the appropriate correction for the entropy change associated with the electrode reaction. The details associated with this correction are described in the following discussion.

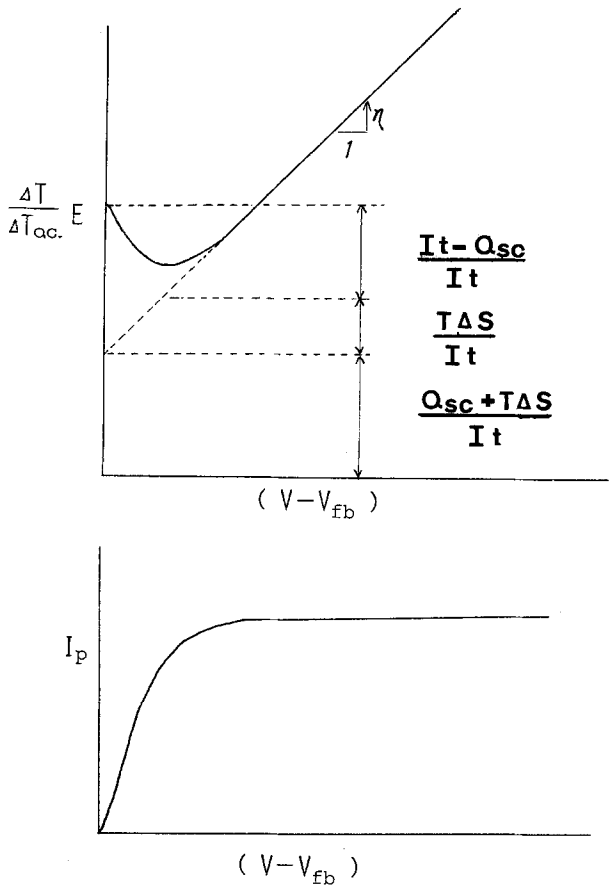

Fig. 8. (Top) Theoretical behavior of the photothermal signal *vs.* potential according to Eq. [12]. (Bottom) Photocurrent *vs.* potential.

Discussion

To illustrate the use of the Eq. [12] in obtaining the quantum and energy efficiencies, the results shown in Fig. 6 and 7 are replotted in Fig. 9 and 10, in which the ordinate is $E\frac{\Delta T}{\Delta T_{oc}}$ and the abscissa is $(V - V_{FB})$.

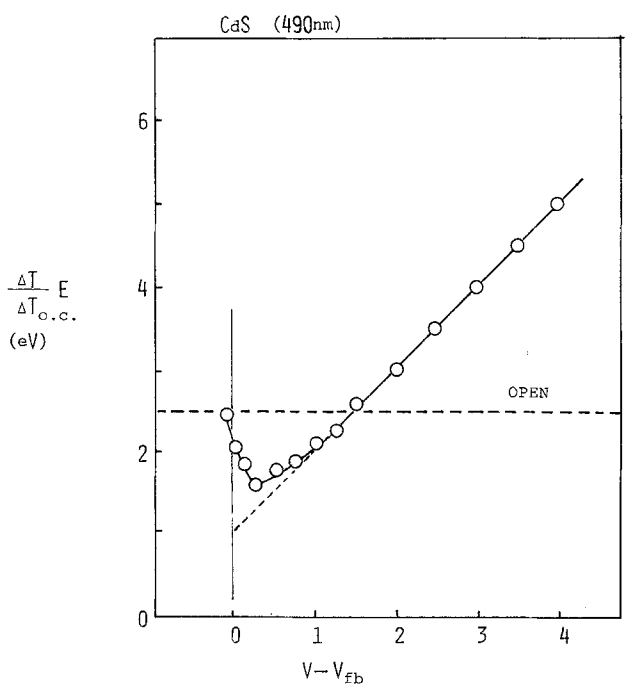

Fig. 9. Normalized photothermal signal *vs.* potential from the flatband potential of the CdS electrode.

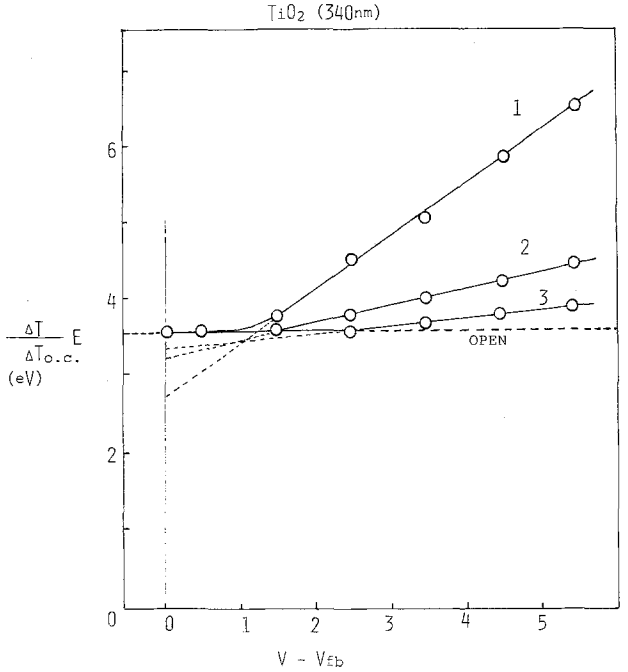

Fig. 10. Normalized photothermal signal *vs.* potential from the flatband potential of the TiO_2 electrodes. TiO_2 single crystals were treated in the vacuum atmosphere, No. 1: for 3 hr at 650°C; No. 2: for 3 hr at 550°C; No. 3: for 4 hr at 800°C.

For the CdS/$Fe(CN)_6^{3-}$, $Fe(CN)_6^{4-}$ system the temperature increase of 1.7×10^{-2}°C which was measured at open circuit corresponds to $E = 2.5$ eV because 490 nm monochromatic light was used to excite the CdS electrode (Fig. 9). In the limiting photocurrent region, we find a straight line with a slope equal to 1.0. This means that the quantum efficiency of the photoreaction on the CdS electrode is unity, which is similar to the value found from the photocurrent and the calibrated light intensity (number of photons striking the electrode). From the intercept of the Y-axis obtained by extrapolating the linear portion of the curve to the flatband potential, we can calculate the energy efficiency of the photosemiconductor reaction, if entropic heat attributable to the electrode reaction ($T\Delta S$ or the Peltier heat) can be obtained. The behavior known as the electrochemical Peltier effect (*i.e.*, the entropy change at the electrode surface) has been investigated by Tamamushi (20). This effect can be attributed to three contributions: the entropy of the electrode reaction, the entropy attributed to the migration of ions and electrons, and the entropy caused by electrochemical polarization. Tamamushi investigated this effect during a study of the electrochemistry of the $K_4Fe(CN)_6/K_3Fe(CN)_6$ redox couple at a gold electrode. Cooling was observed during the oxidation step and heating occurred during reduction at potentials near the equilibrium potential; this can be attributed primarily to an entropy effect of the electrode reaction. This same effect must also be included in the photochemical reaction on the CdS surface.

To obtain the appropriate corrections in our thermal measurements, the electrochemistry of the $K_4Fe(CN)_6/K_3Fe(CN)_6$ couple at a platinum electrode was studied. The entropy effect was similar to that found by Tamamushi in which cooling occurred under the anodic polarization and an equal amount of heating occurred under the cathodic polarization. It is only necessary to make this further correction for the electrochemical reaction entropy near the equilibrium potential, because the polarization effect was already included in the $\eta_q(V - V_{FB})$ term in Eq. [8] and the migration effect would be negligible (the solution and the CdS electrode, resistivity = 1-2 Ω/cm, were both highly conductive).

In this same solution, heating was also observed during the dark cathodic reaction on the CdS electrode under nitrogen bubbling. The amount of heating was 3.4×10^{-3}°C (which corresponds to 0.5 eV in this case), when a cathodic current of 850 μA (which was the same as the saturated photoanodic current) was passed for 20 sec. Therefore, assuming that the photoanodic reaction entropy is equal but opposite to this entropy (from the results on the platinum electrode), the endothermic entropy change on the CdS photoanode for a 20 sec light pulse was determined to be 0.5 eV.

The value of the intercept in Fig. 9, $(Q_{sc} + T\Delta S)/It$, was 1.0 eV. So, taking $T\Delta S/It = 0.5$ eV (endothermic), we find $Q_{sc}/It = 1.5$ eV. In this case (490 nm irradiation), the monochromatic energy conversion efficiency is $100 \times EIt - Q_{sc}/EIt = 100 \times 1.0/2.5 = 40\%$. This result is also consistent with the fact that only a fraction of the energy is being utilized for the oxidation of $Fe(CN)_6^{4-}$ to $Fe(CN)_6^{3-}$; *i.e.*, for the whole cell

$$CdS/0.1M\ K_4Fe(CN)_6;\quad 0.001M\ K_3Fe(CN)_6/Pt$$

the maximum cell voltage obtainable is $|V_{FB} - V_{redox}| \simeq 1.0$V, while the energy of the incoming radiation is 2.5 eV (490 nm).

As shown in Fig. 10 for the TiO_2/H_2SO_4 system, three different lines were obtained, with slopes of 0.7, 0.3, and 0.1. These correspond to the quantum efficiencies of the different TiO_2 photoanodes. Again, as in the case of CdS, calculations using the intercepts of these lines can yield the various energy efficiencies. As is obvious from the results in Fig. 10, the photoanode which shows the smallest quantum efficiency (*i.e.*, smaller slope) has the largest intercept (*i.e.*, the lowest energy conversion efficiency). To get the actual energy conversion efficiency, we must again correct for the Peltier entropy effect, which is proportional to the magnitude of the photocurrent. The oxidation on the TiO_2 photoanode was oxygen evolution based on water decomposition. Contrary to the oxidation of $Fe(CN)_6^{4-}$ as mentioned above, oxygen evolution on the electrode showed exothermic heating behavior, mainly due to the entropy of the electrochemical reaction. To make the appropriate corrections for this entropy effect the reduction of $K_3Fe(CN)_6$ was examined at TiO_2 and platinum and the results compared to those observed during the oxidation of water at platinum. In this manner the magnitude of the entropy effect occurring during the photo-oxidation at TiO_2 could be estimated. When the anodic photocurrent was 1.8 mA (No. 1 in Fig. 10), it was found that the entropy effect corresponded to 0.5 eV. Therefore for electrode 1, since $E = 3.5$ eV (340 nm), $Q_{sc} + T\Delta S/It = 2.7$ eV (from the intercept), and $T\Delta S/It = -0.5$ eV (the entropy effect). Therefore, $Q_{sc}/It = 2.2$ eV. The energy conversion efficiency can be determined as

$$100 \times \frac{EIt - Q_{sc}}{EIt} = 100 \times 1.3/3.5 = 37\%$$

The fraction of the photon energy that is not used in the oxidation of the redox species is dissipated as heat via two possible mechanisms as shown in Fig. 11. The first mechanism, (a), represents the filling of a valence band hole by the reduced species in solution to produce a vibrationally excited species. This energy is quickly dissipated in the solution as heat. The second mechanism, (b), represents the isoenergetic electron transfer from the reduced species in solution to a surface state which then recombines with a hole in the valence band of the semiconductor, with the heat dissipated in the semiconductor itself. However, at this time we can not distinguish the difference between heat produced in solution or heat on the electrode itself. Therefore neither mechanism can be verified using only the temperature measurement.

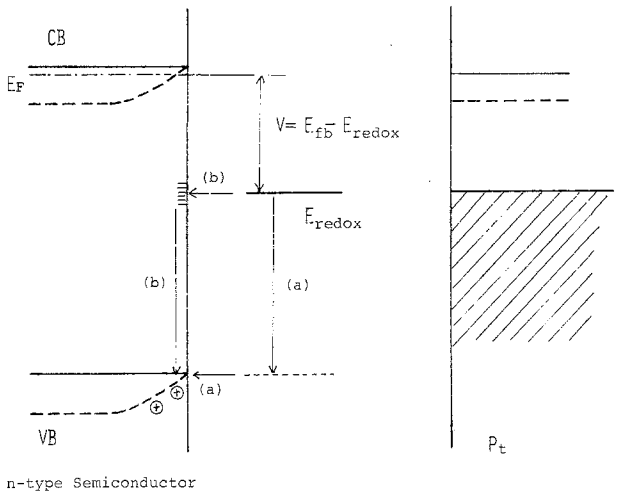

Fig. 11. Maximum open-circuit photopotential and heat dissipation mechanism.

Conclusion

By *in situ* temperature measurements of the semiconductor electrode, the quantum and energy efficiency of the electrode reaction could be obtained. The advantage of this type of measurement lies in the fact that it is a relative measurement and therefore does not depend upon knowing the light intensity. This eliminates the need for calibration of the excitation source and establishes a method by which results in different laboratories can be compared more easily. A disadvantage of the technique is that the precision of the measurements ($\sim \pm 1\%$) limits its use to the more efficient systems.

In considering the efficiencies obtained in this manner one should note that the results presented refer to the efficiency of the electrode reaction and not to the entire photoelectrochemical cell. In this work no attention was given to the reaction occurring at the counterelectrode or to whether the cell was photovoltaic or photosynthetic. In order to treat the entire system thermal measurements during the cell reaction would be necessary. Such measurements could be carried out in a manner similar to that described above or by placing the entire photoelectrochemical cell in a photocalorimeter and measuring the overall thermal change of the cell resulting from illumination. By using the former method both the electrode and cell efficiencies could be determined while calorimetric techniques would only yield the cell efficiency.

Acknowledgment

The support of this research by the National Science Foundation and the U.S. Army Research Office—Durham is gratefully acknowledged.

Manuscript submitted June 18, 1979; revised manuscript received Oct. 19, 1979.

Any discussion of this paper will appear in a Discussion Section to be published in the December 1980 JOURNAL. All discussions for the December 1980 Discussion Section should be submitted by Aug. 1, 1980.

Publication costs of this article were assisted by The University of Texas at Austin.

REFERENCES

1. A. Fujishima and K. Honda, *Nature*, **238**, 37 (1972).
2. A. Fujishima, K. Kohayakawa, and K. Honda, *This Journal*, **122**, 1487 (1975).
3. H. Yoneyama, H. Sakamoto, and H. Tamura, *Electrochim. Acta*, **20**, 341 (1975).
4. K. L. Hardee and A. J. Bard, *This Journal*, **123**, 1027 (1976).
5. A. J. Nozik, *Nature*, **257**, 383 (1975).
6. G. Hodes, D. Cahen, and J. Manassen, *ibid.*, **260**, 312 (1976).
7. H. Gerischer and J. Gobrecht, *Ber. Bunsenges. Phys. Chem.*, **80**, 327 (1976).
8. B. Miller and A. Heller, *Nature*, **262**, 680 (1976).
9. A. B. Ellis, S. W. Kaiser, J. M. Bolts, and M. S. Wrighton, *J. Am. Chem. Soc.*, **99**, 2839 (1977).
10. H. Gerischer, *J. Electroanal. Chem. Interfacial Electrochem.*, **58**, 263 (1975).
11. M. S. Wrighton, A. B. Ellis, P. T. Wolczanski, D. L. Morse, H. B. Abrahamson, and D. S. Ginley, *J. Am. Chem. Soc.*, **98**, 2774 (1976).
12. J. G. Mavroides, D. I. Tchernev, J. A. Kafalas, and D. F. Kolesar, *Mater. Res. Bull.*, **10**, 1023 (1975).
13. Y. G. Chai and W. W. Anderson, *Appl. Phys. Lett.*, **27**, 183 (1975).
14. M. S. Wrighton, D. S. Ginley, P. T. Wolczanski, A. B. Ellis, D. L. Morse, and A. Linz, *Proc. Natl. Acad. Sci. U.S.A.*, **72**, 1518 (1976).
15. A. B. Ellis, S. W. Kaiser, and M. S. Wrighton, *J. Am. Chem. Soc.*, **98**, 6855 (1976).
16. G. H. Brilmyer, A. Fujishima, K. S. V. Santhanam, and A. J. Bard, *Anal. Chem.*, **49**, 2057 (1977).
17. A. Fujishima, G. H. Brilmyer, and A. J. Bard, in "Semiconductor Liquid-Junction Solar Cells," A. Heller, Editor, p. 172, The Electrochemical Society Softbound Proceedings Series, Princeton, N.J. (1977).
18. D. Cahen, *Appl. Phys. Lett.*, **33**, 810 (1978).
19. J. M. Sherfey and A. Brenner, *This Journal*, **105**, 665 (1958).
20. R. Tamamushi, *J. Electroanal. Chem. Interfacial Electrochem.*, **45**, 500 (1973); **65**, 263 (1975).